19 Feb 2019

Characterization and Quantification of Highly Sulfated Glycosaminoglycan Isomers by Gated-Trapped Ion Mobility Spectrometry Negative Electron Transfer Dissociation MS/MS

Juan Wei

Jiandong Wu
Missorui University of Science and Technology, jiandong.wu@mst.edu

Yang Tang

Mark E. Ridgeway

et. al. For a complete list of authors, see https://scholarsmine.mst.edu/che_bioeng_facwork/1415

Recommended Citation

J. Wei et al., "Characterization and Quantification of Highly Sulfated Glycosaminoglycan Isomers by Gated-Trapped Ion Mobility Spectrometry Negative Electron Transfer Dissociation MS/MS," *Analytical Chemistry*, vol. 91, no. 4, pp. 2994 - 3001, American Chemical Society, Feb 2019.
The definitive version is available at https://doi.org/10.1021/acs.analchem.8b05283

analytical chemistry

Article

Cite This: *Anal. Chem.* 2019, 91, 2994−3001

pubs.acs.org/ac

Characterization and Quantification of Highly Sulfated Glycosaminoglycan Isomers by Gated-Trapped Ion Mobility Spectrometry Negative Electron Transfer Dissociation MS/MS

Juan Wei,[†] Jiandong Wu,[†] Yang Tang,[†,‡] Mark E. Ridgeway,[§] Melvin A. Park,[§] Catherine E. Costello,[†,‡] Joseph Zaia,[†] and Cheng Lin*[,†]

[†]Center for Biomedical Mass Spectrometry, Boston University School of Medicine, Boston, Massachusetts 02118, United States

[‡]Department of Chemistry, Boston University, Boston, Massachusetts 02215, United States

[§]Bruker Daltonics, Billerica, Massachusetts 01821, United States

Supporting Information

ABSTRACT: Glycosaminoglycans (GAGs) play vital roles in many biological processes and are naturally present as complex mixtures of polysaccharides with tremendous structural heterogeneity, including many structural isomers. Mass spectrometric analysis of GAG isomers, in particular highly sulfated heparin (Hep) and heparan sulfate (HS), is challenging because of their structural similarity and facile sulfo losses during analysis. Herein, we show that highly sulfated Hep/HS isomers may be resolved by gated-trapped ion mobility spectrometry (gated-TIMS) with negligible sulfo losses. Subsequent negative electron transfer dissociation (NETD) tandem mass spectrometry (MS/MS) analysis of TIMS-separated Hep/HS isomers generated extensive glycosidic and cross-ring fragments for confident isomer differentiation and structure elucidation. The high mobility resolution and preservation of labile sulfo modifications afforded by gated-TIMS MS analysis also allowed relative quantification of highly sulfated heparin isomers. These results show that the gated-TIMS-NETD MS/MS approach is useful for both qualitative and quantitative analysis of highly sulfated Hep/HS compounds in a manner not possible with other techniques.

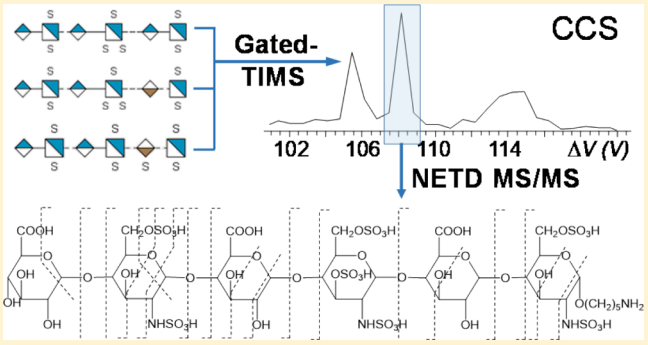

Glycosaminoglycans (GAGs) are linear polysaccharides consisting of disaccharide repeats with alternating amino sugar and hexuronic acid (HexA) or galactose units. Through interaction with their protein binding partners, GAGs are involved in many biological processes including cell signaling, inflammation, cell proliferation, and tumor metastasis.[1−12] Heparin (Hep) and heparan sulfate (HS) are GAGs with a high degree of sulfation and among the most acidic biomolecules found in nature. The electrostatic interaction between Hep/HS and protein ligands is modulated by their sulfation pattern and plays a key role in their biological functions. For example, binding between antithrombin and a pentasaccharide sequence containing a critical 3-*O* sulfation on the central glucosamine (GlcN) residue is essential for the anticoagulation activity of Hep/HS.[13,14] Heparins also mediate recognition between fibroblast growth factors (FGFs) and their receptors, thereby regulating cell proliferation.[15−18] Whereas FGF-2 preferentially interacts with tetra- and hexasaccharide sequences containing the -IdoA2S-GlcNS- motif (IdoA = iduronic acid), FGF-1 has a strong affinity to the -IdoA2S-GlcNS6S- motif. Heparins containing 6-*O* sulfation display anti-inflammatory properties by interfering with P- and L-selectin-initiated cell adhesion.[5] Despite the strong correlation between the GAG structures and their biological functions, subtle structural differences are often difficult to track, and full characterization of GAGs, especially the highly sulfated Hep/HS glycans, remains a significant analytical challenge.

Although all Hep/HS saccharides share the same HexA(1 → 4)-GlcN(α1 → 4)- disaccharide sequence repeats, the number of Hep/HS structures is multiplied by the variation in the number of repeating units, the hexuronic acid stereochemistry, and the pattern of *N*-acetylation and sulfation, resulting in tremendous structural diversity and the common occurrence of isomers.[19] GAG analysis often requires enzymatic digestion or chemical depolymerization to break down polysaccharide chains into shorter oligosaccharides with degrees of polymerization (dp) ranging from dp2 to dp20. The Hep/HS digests are then analyzed by mass spectrometry (MS), usually in conjunction with liquid chromatography (LC). The extent and pattern of sulfation in the original Hep/HS chains can be estimated by relative quantitation of all oligosaccharides.

Received: November 14, 2018
Accepted: January 16, 2019
Published: January 16, 2019

DOI: 10.1021/acs.analchem.8b05283
Anal. Chem. 2019, 91, 2994−3001

Isomeric Hep/HS structures may be separated by capillary electrophoresis (CE)[20−22] or by LC, including reversed phase-ion pairing (RP-IP) chromatography, hydrophilic interaction liquid chromatography (HILIC), strong anion exchange (SAX) chromatography, and porous graphitized carbon (PGC) chromatography.[23−27] Among these, SAX offers the highest isomer resolving power but is incompatible with direct MS analysis due to the high concentration of nonvolatile salt used in the elution buffer. An alternative, volatile salt cetyltrimethylammonium (VSCTA)-SAX, uses the buffer ammonium bicarbonate that can be easily removed by evaporation, thus allowing effective subsequent analysis by offline electrospray MS. Meanwhile, superior isomer resolution of HS oligosaccharides was recently demonstrated by Miller et al. with online PGC-LC-MS/MS analysis.[27] However, there are concerns over PGC column stability and reproducibility and the formation of ammonium adducts leading to increased precursor heterogeneity.

Ion mobility spectrometry[28] has emerged as a powerful alternative for separation of isomeric structures, including GAG isomers.[29−35] IMS complements LC in that it is a postionization, gas-phase separation method, wherein analyte ions are sorted on the basis of their size, charge, and shape. Isomers may differ in collisional cross section (CCS) and, therefore, ion mobilities, depending on their gas-phase conformations. IMS analysis is generally faster than LC and can be easily coupled to MS. Moreover, the CCS of an analyte ion is an additional property which can be used for its identification.

Significant progress in GAG structural characterization has been made through the development of electron activated dissociation (ExD) tandem MS (MS/MS) methods.[36−42] In particular, electron detachment dissociation (EDD)[37,38] and negative electron transfer dissociation (NETD)[39−42] are capable of generating extensive glycosidic and cross-ring cleavages while preserving labile sulfate modifications in highly sulfated GAGs, thus allowing sequence determination and sulfation site localization. Differentiation of C5 epimers, IdoA and GlcA (glucuronic acid), by EDD and NETD has also been demonstrated.[36,43] EDD MS/MS has been used in conjunction with high-field asymmetric-waveform ion mobility spectrometry (FAIMS) to separate and characterize epimeric HS tetrasaccharides.[32] However, FAIMS does not provide CCS measurement, as it separates ions on the basis of their differential mobilities in strong and weak electric fields. The applications of FAIMS are restricted by its relatively low sensitivity and limited peak capacity that result from diffusion and harsh discrimination against high-mobility ions.[44]

EDD and NETD MS/MS analyses are performed on a time scale longer than the conventional drift-time IMS separation. It is possible to couple IMS separation with slower analysis methods when the IMS device is used as a mobility filter.[45,46] Trapped ion mobility spectrometry (TIMS)[47,48] offers high mobility resolution and ion transmission efficiency and has shown great promise in isomer separations.[49−52] Successful coupling of TIMS to Fourier-transform ion cyclotron resonance (FTICR) MS has been achieved under the selected accumulation (SA)-TIMS mode and applied to characterization of isomeric glycan mixtures.[53] However, SA-TIMS requires extended ion storage time in the TIMS analyzer, leading to significant ion heating and is therefore not suitable for analysis of labile compounds or compounds whose conformers may interconvert during the storage time. Such limitation may be overcome by gated-TIMS where ions of a given mobility are selected by an electrical gate and accumulated in a low-pressure collision cell.[54,55] Here, we present our initial results on the gated-TIMS coupling to NETD MS/MS and demonstrate its utility for characterization and quantification of isomeric Hep/HS oligosaccharides.

EXPERIMENTAL SECTION

Materials. GAG standards, GlcA-GlcNAc6S-IdoA-GlcNAc6S-$(CH_2)_5$-NH_2 (Compound **1**), GlcA-GlcNAc-IdoA2S-GlcNAc6S-$(CH_2)_5$-NH_2 (Compound **2**), GlcA-GlcNS6S-GlcA-GlcNS3S6S-GlcA-GlcNS6S-$(CH_2)_5$-NH_2 (Compound **3**), GlcA-GlcNS6S-GlcA-GlcNS3S6S-IdoA-GlcNS6S-$(CH_2)_5$-NH_2 (Compound **4**), and GlcA-GlcNS6S-GlcA-GlcNS6S-IdoA2S-GlcNS6S-$(CH_2)_5$-NH_2 (Compound **5**) were synthesized by the Boons's group at the University of Georgia as described previously;[56] their structures and symbol nomenclature for glycans (SNFG) representations are shown in Figure S1. All GAG standards were alkylated at the reducing end via an α-linkage to facilitate fragment assignment and eliminate anomerism-induced conformational heterogeneity. All other chemicals were purchased from Sigma-Aldrich (St. Louis, MO, USA).

Gated-TIMS-MS and Gated-TIMS-NETD MS/MS Analyses. All experiments were carried out on a Bruker 12-T solariX FTICR mass spectrometer equipped with a prototype TIMS device (Bruker Daltonics, Billerica, MA). GAGs were dissolved in 75:25 water/acetonitrile with 0.1% formic acid to a concentration of around 5 pmol/μL except for the quantitative analysis, where Compounds **3** and **4** were mixed at ratios of 20:1, 10:1, 2:1, 1:1, 1:2, 1:10, and 1:20, respectively, with concentrations ranging from 5 to 100 pmol/μL. Around 5 μL of sample was loaded into a pulled glass capillary tip with a 1 μm orifice diameter and introduced into the mass spectrometer via static nanoelectrospray. The schematic of the TIMS device and the principle of the gated-TIMS operation were described in detail previously.[54] Briefly, ions entering the TIMS funnel were trapped radially by an RF potential (190 Vpp) and axially by an electric field gradient (EFG) at positions where their drift velocity equals the carrier gas flow velocity. Following a 9 ms trapping event, the strength of the axial electric field was gradually decreased by ramping the TIMS analyzer entrance potential from 250 to −50 V to allow elution of ions in the order of ascending mobilities. A downstream ion gate was pulsed open to allow only ions of selected mobility to pass through and be accumulated in the collision cell. For MS/MS analysis, ions of a given mobility were mass selected by a quadrupole before entering the collision cell. The drift gas (nitrogen) pressure was regulated between 2.5 and 2.7 mbar, depending on the mobility resolution needed. A mixture of perfluoroalkyl phosphazine standards (Agilent Technologies, Santa Clara, CA, USA) was used to generate the mobility calibration curve for CCS calculation. For NETD experiments, fluoranthene cation radicals were generated by a chemical ionization source with argon as the buffer gas. A reagent accumulation time of 200 to 500 ms and a reaction time of 50 to 100 ms were typically used.

Data Analysis. All spectra were processed by DataAnalysis 4.4 (Bruker, Bremen, Germany) and interpreted manually assisted by GlycoWorkbench.[57] Fragments were annotated according to the Domon and Costello nomenclature.[58]

DOI: 10.1021/acs.analchem.8b05283
Anal. Chem. 2019, 91, 2994−3001

RESULTS AND DISCUSSION

Reduced Ion Heating during Gated-TIMS Analysis. TIMS is commercially available only on time-of-flight MS instruments, as separation occurs on the millisecond time scale, and thus is more easily coupled to a fast mass analyzer. TIMS coupling to slower analysis methods, such as ExD-FTICR MS/MS, was first accomplished by modifying the axial EFG profile to include an electric field plateau for selective accumulation of ions with the desired mobility inside the TIMS tunnel, as implemented in SA-TIMS.[53] However, prolonged ion accumulation during SA-TIMS (hundreds of milliseconds) can result in the radial ion cloud expansion and multipole storage assisted dissociation (MSAD) that has been investigated by the groups of Håkansson and Hofstadler.[59−61] In contrast, gated-TIMS involves a short ion accumulation time in the TIMS tunnel (around 10 ms), and multiple collision cell fills are used to increase the abundance of ions of the desired mobility and to match the time scale of FTICR MS analysis. The collision cell has a much higher space charge capacity and lower gas pressure ($\sim 10^{-3}$ mbar), and consequently, ion storage here minimizes MSAD. Suppression of lower-abundance ions of interest in the collision cell is not an issue following mobility selection and m/z filtering.

The advantage of gated-TIMS over SA-TIMS for analysis of labile compounds is illustrated in Figures 1 and S2, showing the influence of the TIMS accumulation time on the extent of sulfo losses from a highly sulfated HS hexasaccharide (Compound **3**). Although extensive sulfo losses were observed when the TIMS accumulation time exceeded 100 ms (Figure 1d,e), sulfo loss was negligible with a 10 ms TIMS accumulation time even after 600 cycles of collision cell fills (Figure 1f). It appears that the sulfo losses that did occur took place primarily inside the TIMS tunnel, as the majority of sulfo-loss fragment ions did not coelute with the precursor (Figure S2c,d, bottom panels). Multiple peaks observed in the extracted ion mobiligrams (EIMs) of fragments may have resulted from loss of sulfo group(s) from different sulfation sites and/or the presence of multiple conformers. Another advantage of gated-TIMS is that the reduced ion storage time minimizes conformational changes. Conformational heating at longer fill/trap times was previously reported for TIMS-TOF MS analysis of ubiquitin ions.[62] Whereas a single peak existed in the EIMs of the $[M - 3H]^{3-}$ species (eluting at 108 V) when the TIMS accumulation time was 10 ms, a second peak with a higher CCS was observed at 110 V when the accumulation time exceeded 50 ms, likely due to heating and unfolding (Figure S2, top panel). Thus, gated-TIMS is well-suited for analysis of highly sulfated GAGs, as it preserves labile modifications and minimizes conformational heterogeneity.

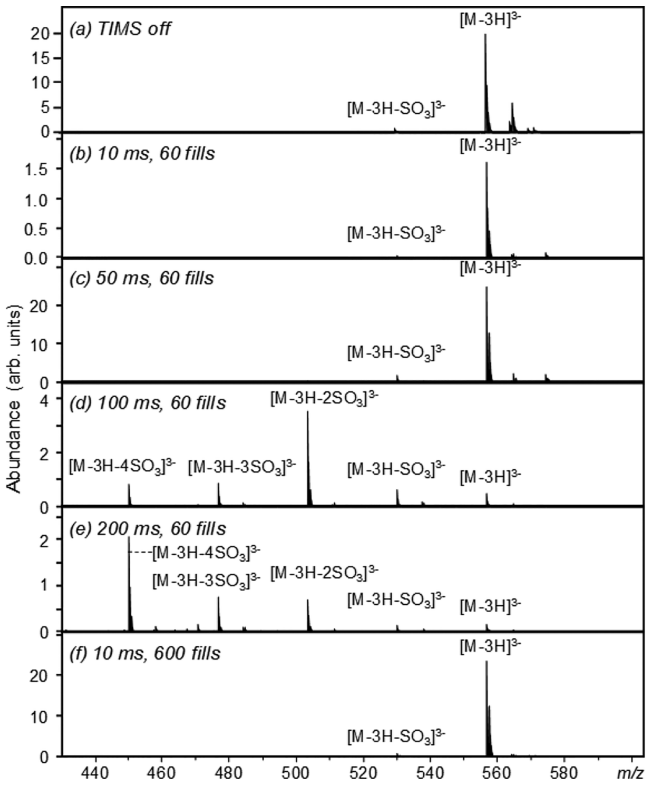

Figure 1. (a) A mass spectrum of Compound **3** acquired in the transmission mode (TIMS off); (b−f) averaged mass spectra of Compound **3** acquired with different TIMS accumulation times and number of collision cell fills.

Separation of GAG Isomers by Gated-TIMS. Apart from facile sulfo losses, challenges in MS analysis of GAGs may also arise due to the presence of precursor ions in a range of charge states and cation-adducted forms. Distribution of analytes into multiple species dilutes the signal and complicates the MS analysis. Ammonium adduction is very common in LC-MS analysis of GAGs because of the use of ammonium salt in the elution buffer. In contrast, for IM-MS analysis with direct infusion, the ionization conditions, including the pH and composition of the ESI solution, can be easily manipulated to control the charge state distribution and cation adduction. Figure S3 shows that the addition of 0.1% formic acid significantly reduced cation adduction. The analyte charge states also affect the performance of mobility separation and the NETD spectral quality. Though the NETD efficiency increases with the precursor ion charge state, GAG isomers in higher charge states tend to produce more extended and thus similar gas-phase structures that are difficult to resolve by IMS. Rapid survey scans at relatively low mobility resolution may be first performed to identify the best conditions for separation of isomeric structures. The instrument parameters can then be tuned for higher-resolution scans within targeted mobility ranges. Typical gated-TIMS operating parameters are summarized in Table S1.

Survey scans of Compounds **1** and **2** (Figure S4) suggested that these two tetrasaccharide (dp4) isomers with a moderate degree of sulfation may be resolved in both 2− and 3− charge states. A high-resolution scan was then performed for the 3− charge state because of its potential to generate more informative NETD spectra. Baseline resolution was achieved for this pair of isomers that differ by the location of one sulfo group (Figure 2a). Likewise, three hexasaccharide (dp6) isomers with a high degree of sulfation, differing in either the location of one sulfo group (Compounds **4** and **5**) or the epimeric configuration of a single uronic acid residue (Compounds **3** and **4**), were fully resolved in the 3− charge state (Figure 2b). In contrast, higher charge states (4− and 5−) of these dp6 isomers have similar mobilities and cannot be fully resolved (Figure S5).

The x-axis of the EIMs shown displays the elution voltage or the potential drop across the TIMS analyzer ($\Delta V = V_{\text{tunnel}} - V_{\text{exit funnel}}$) at the time of elution. The CCS value of each compound (Figure 2, bottom panel) could be calculated on the basis of its elution voltage using a calibration curve

DOI: 10.1021/acs.analchem.8b05283
Anal. Chem. 2019, 91, 2994−3001

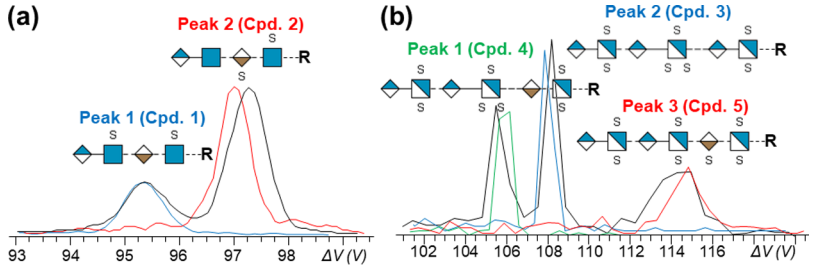

[M-3H]$^{3-}$	CCS (N_2, Å^2)
Compound 1	334.6 ± 0.4
Compound 2	342.7 ± 0.5

[M-3H]$^{3-}$	CCS (N_2, Å^2)
Compound 3	362.3 ± 0.2
Compound 4	354.3 ± 1.0
Compound 5	379.9 ± 0.6

Figure 2. Gated-TIMS separation of two sets of dp4 and dp6 isomers. (a) EIMs ($[M - 3H]^{3-}$) of Compound **1** (blue trace), Compound **2** (red trace), and their mixture (black trace); (b) EIMs ($[M - 3H]^{3-}$) of Compound **3** (blue trace), Compound **4** (green trace), Compound **5** (red trace), and their mixture (black trace). Averaged CCS values of each compound from three measurements are listed with their standard deviations below the EIMs. R = $C_5H_{10}NH_2$.

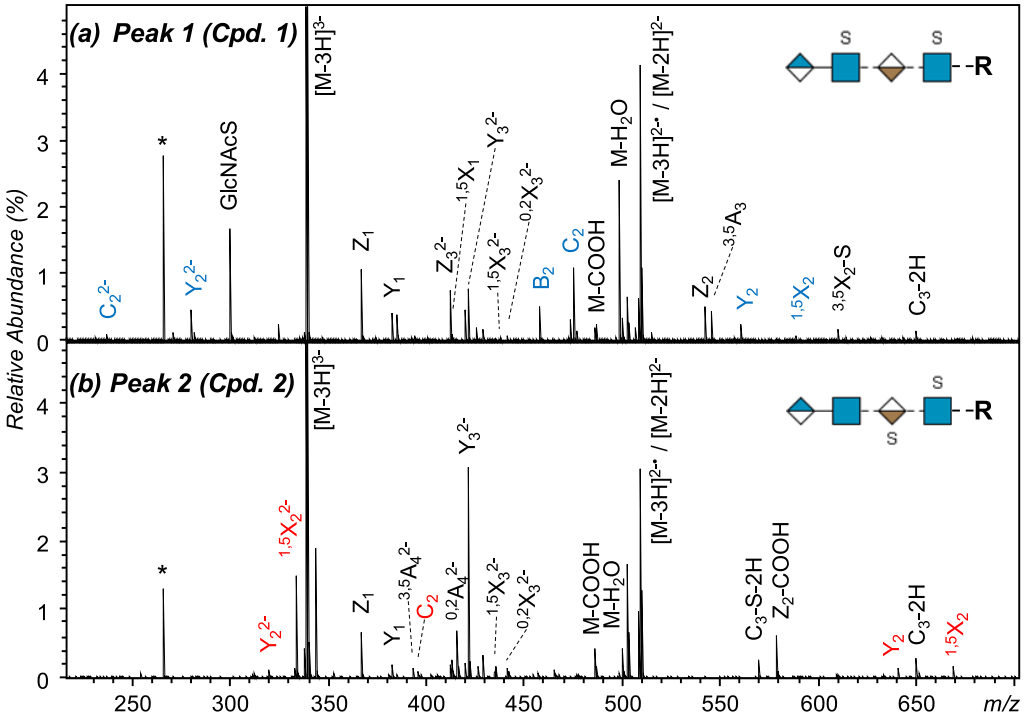

Figure 3. Gated-TIMS NETD MS/MS analysis of a mixture of Compounds **1** and **2** in the 3− charge state. (a, b) NETD spectra of peak 1 and peak 2, respectively, in Figure 2a. Asterisks mark the electronic noise. Measured m/z values for assigned peaks are shown in Tables S2 and S3. R = $C_5H_{10}NH_2$.

established with a series of compounds of known mobilities.[47] The CCS of an analyte is a fixed value when measured under the same conditions and can be stored in a database for future reference. Here, the high mobility resolving power offered by gated-TIMS was essential for resolution of isomers with CCS values differing by as little as 2%. Note that the elution voltages of some isomers, when analyzed in the mixture, were slightly different from their respective elution voltages, when analyzed individually. These small shifts likely resulted from the run-to-run pressure fluctuation inside the TIMS tunnel but were generally less than 0.5%.

Gated-TIMS NETD MS/MS Analysis of dp4 Isomers. Unlike SA-TIMS, ions of the desired mobility occupy only a small section of the mobility analyzer during the gated-TIMS operation. External accumulation of ions of interest via multiple collision cell fills may be performed to increase the ion abundance for effective ExD analysis. The impact of multiple fill cycles on the analysis speed can be minimized with accumulation during detection (ADD), where ion accumulation is performed in parallel with MS analysis of the previous ion packet in the ICR cell. In the analyses whose results are shown here, 600 to 900 fill cycles were used prior to NETD. For structural characterization, each mobility- and mass-selected isomer was subjected to NETD in the collision cell.

Figure 3 shows the NETD tandem mass spectra of the two TIMS-isolated dp4 isomers, and their fragmentation patterns are shown in Figure S6. Peak assignment was facilitated by the high-mass accuracy FTICR MS measurement and the presence of the reducing-end aminopentyl group. Lists of all assigned fragments can be found in Tables S2 and S3. NETD generated

DOI: 10.1021/acs.analchem.8b05283
Anal. Chem. 2019, 91, 2994−3001

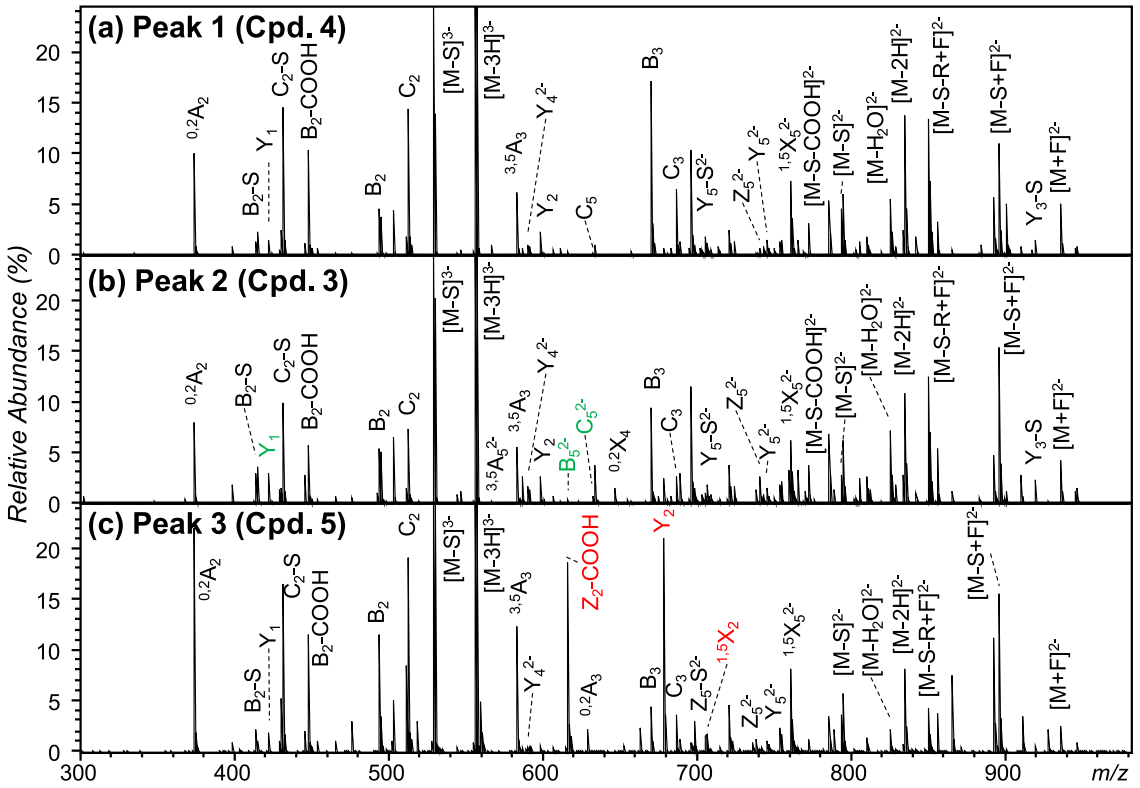

Figure 4. Gated-TIMS NETD MS/MS analysis of a mixture of Compounds **3**, **4**, and **5** in the 3− charge state. (a−c) NETD spectra of peaks 1, 2, and 3, respectively, in Figure 2b. Sulfo losses are labeled as − S; fluoranthene adducts are indicated by + F; the loss of the aminopentyl group is marked by − R. Measured *m*/*z* values for assigned peaks are shown in Tables S4−S6.

many glycosidic and cross-ring fragments without sulfo losses, including several fragment ions unique to each isomer (highlighted in color). In both spectra, the presence of Y_1 and Z_1 ions containing one sulfo group may be used to assign one sulfation site to the reducing-end GlcNAc residue. The second sulfation site may be localized to the internal GlcNAc residue for isomer 1, on the basis of the mass difference between its Y_3^{2-} (or Z_3^{2-}) fragment ion (with 2S) and Y_2 (or Z_2) fragment ion (with 1S) (Figure 3a), and to the internal IdoA residue for isomer 2, on the basis of the mass difference between its C_2 (with no S) and C_3-2H (with 1S) ions (Figure 3b). The sulfation site at the terminal GlcNAc residue can be defined at the 6-*O* position in each isomer, on the basis of the observation of a $^{3,5}A_4$ ion with two sulfo groups; likewise, the second sulfo group in isomer 1 can be assigned to the 6-*O* position of the internal GlcNAc residue, on the basis of the presence of a $^{3,5}A_2$ ion with one sulfo group. Definitive evidence for the exact location of the sulfo group on the IdoA residue of isomer 2 is not present in the spectrum shown here, but this sulfo group is presumed to be located at the 2-*O* position on the basis of known biosynthetic pathways. Thus, peaks 1 and 2 in the EIM of the dp4 mixture can be assigned to Compounds **1** and **2**, respectively.

Gated-TIMS NETD MS/MS Analysis of Highly Sulfated dp6 Isomers. Characterization of the dp6 mixture presents a bigger challenge. First, it is difficult to achieve complete deprotonation on these highly sulfated compounds, with the result that proton-mediated facile sulfo losses can occur easily during ionization, mobility analysis, and ion transfer. Second, the presence of many sulfate and carboxyl groups resulted in a broad charge state distribution and the formation of many sodiated and ammonium-adducted forms. This complicates subsequent MS/MS analyses. Third, although it is preferable to characterize precursor ions in higher charges states due to their higher NETD efficiency, these dp6 isomers could not be fully resolved in 4− and 5− charge states (Figure S5). To overcome these challenges, the instrument parameters and the ESI solvent composition had to be optimized to minimize cation adduction (Figure S3) and sulfo losses, and then, the 3− charge state was chosen for NETD analysis, as all three isomers could be mobility resolved in this charge state.

The NETD spectra of the mobility-selected dp6 isomers are shown in Figure 4a−c, and their fragmentation patterns are shown in Figure S7. Lists of all assigned fragments can be found in Tables S4−S6. In the NETD spectra of peaks 1 and 2 (Figure 4a,b), the Y_2 ions contain only two sulfate groups. This, along with the presence of Y_3 and Z_3 ions with five sulfate groups, suggests that the second GlcN residue is fully sulfated. In contrast, in the NETD spectrum of peak 3 (Figure 4c), the mass difference between its Y_1 (with 2 S) and Y_2 (with 3 S) ions indicates that the HexA residue near the reducing end is singly sulfated, agreeing with the structure of Compound **5**. This assignment is confirmed by the presence of high-abundance Z_2-COOH, $^{1,5}X_2$ ions with three sulfate groups, and a B_5^{2-} fragment with five sulfate groups. Thus, it is relatively easy to distinguish the sulfation positional isomer, Compound **5** from Compounds **3**/**4**, on the basis of their NETD spectra.

Distinction between the other two compounds, presumably the stereoisomeric Compounds **3** and **4**, is more difficult. For both isomers, it is possible to locate all sulfation sites on the basis of the presence of complete series of glycosidic fragments and $^{3,5}A$ and $^{0,2}A$ ions at the first and third GlcNAc residues (Figure S7). Although MS is often considered blind to

DOI: 10.1021/acs.analchem.8b05283
Anal. Chem. 2019, 91, 2994−3001

chirality, diastereomers, such as epimeric isomers, may sometimes be differentiated by MS/MS on the basis of unique fragmentation patterns associated with each stereochemical configuration.[36,38,63−65] Amster and co-workers showed that the C5 uronic acid stereochemistry near the reducing end in HS tetrasaccharides may be determined by EDD MS/MS, on the basis of the differential ratio (DR), DR = log(1/3(Σ(B_3,Y_1,C_2,Z_2))/(Σ(Y_2,$^{1,5}X_2$))), where a positive DR value is associated with GlcA and a negative value, with IdoA.[36] Even though this strategy cannot be directly applied to determine the epimeric configuration in the compounds studied here, because of the difference in the chain length, charge state, and the fragmentation method employed, the DR value may still be used for differentiation. Here, the $^{1,5}X_2$ ions are not observed, and the Y_2 ions have similar abundances, whereas fragments resulting from glycosidic cleavages at the reducing end side of the epimeric center, namely, Y_1, Z_1, B_5^{2-}, and C_5^{2-} ions (labeled in green in Figure 4b), are about 2 to 5 times more abundant in the NETD spectrum of peak 2 than in that of peak 1 (Figure S8). As peaks 2 and 1 correspond to $GlcA_5$-containing Compound **3** and $IdoA_5$-containing Compound **4**, respectively, on the basis of the elution time observed for individual dp6 standards, it appears that glycosidic cleavages on the reducing end side of GlcA are more prevalent than those next to IdoA. Moreover, the abundance of the cross-ring fragment, $^{0,2}X_4^{2-}$, is eight times greater in Figure 4b than in Figure 4a, suggesting that the epimeric configuration can influence fragmentation distant from the stereochemical center, potentially providing additional information for epimer differentiation. Thus, it is possible to assign these two stereoisomers by comparing either their CCS values to those of the standards (Figure 2b) or their NETD fragmentation patterns. Here, gated-TIMS NETD MS/MS analysis provided both CCS values and the fragmentation data to enable confident identification.

Relative Quantification of Isomers by Gated-TIMS FTICR MS. Characterization of a highly heterogeneous GAG mixture via a bottom-up approach requires not only identification of oligosaccharides present in its digest but also their relative quantification. However, highly sulfated GAG isomers are difficult to resolve chromatographically, and facile sulfo losses further complicate the analysis. We showed earlier that gated-TIMS could resolve highly sulfated Hep/HS isomers with negligible sulfo losses. Here, two stereoisomers, Compounds **3** and **4**, were mixed at ratios ranging from 20:1 to 1:20 and subjected to nanoESI-gated-TIMS FTICR MS analysis. With a mobility resolution of around 200, these two compounds were baseline resolved in the 3− charge state. Figure 5 shows that the peak area ratio, A3/(A3 + A4), scales linearly with the fraction of Compound **3** in the mixture, C3/(C3 + C4), thus demonstrating the feasibility of using gated-TIMS MS for relative quantification of GAG isomers. In conjunction with the NETD MS/MS analysis, it is now possible to achieve both identification and quantification of highly sulfated GAG isomers.

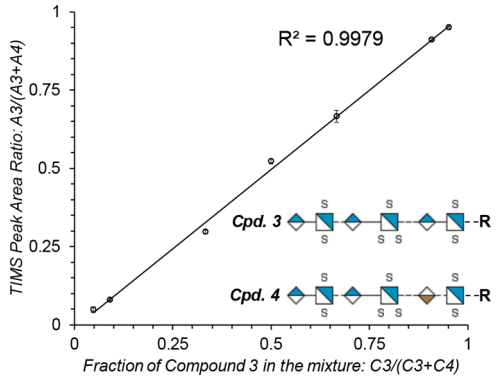

Figure 5. Relative quantification of two dp6 stereoisomers. The peak area ratio, A3/(A3 + A4), was averaged over three technical replicates and plotted against the ratio of the concentration of Compound **3** over the total concentration, C3/(C3 + C4). Error bars show the standard deviations of three measurements (generally less than 2%). Data used to generate this plot can be found in Table S7. R = $C_5H_{10}NH_2$.

CONCLUSIONS

To meet the challenges of GAG analysis, a high-resolution ion mobility separation technique, gated-TIMS, was integrated with NETD, a dissociation method that preserves labile modifications, and high mass resolution FTICR MS, for characterization of highly sulfated GAG isomers. Compared with SA-TIMS, gated-TIMS showed superior performance in preserving the labile sulfo groups, while retaining the ability to resolve isomeric structures and was also compatibile with FTICR analysis. Synthetic dp4 and dp6 standards, including sulfation positional isomers and IdoA/GlcA stereoisomers, could be baseline resolved by gated-TIMS, and their CCS values could be measured and stored for future reference. Online gated-TIMS NETD MS/MS generated extensive fragmentation with a high degree of sulfo retention for detailed structural characterization, along with many diagnostic fragments for isomer differentiation. Relative quantification of highly sulfated Hep/HS isomers was demonstrated for the first time, aided by the high mobility resolution and the soft analysis conditions of gated-TIMS-NETD MS/MS. Coupling of gated-TIMS with NETD MS/MS appears to be a powerful tool for qualitative and quantitative analysis of highly sulfated GAGs.

ASSOCIATED CONTENT

Supporting Information

The Supporting Information is available free of charge on the ACS Publications website at DOI: 10.1021/acs.analchem.8b05283.

Figure S-1, structures of the synthetic GAG standards used in this study; Figure S-2, EIMs of Compound **3** ($[M - 3H]^{3-}$) and its sulfo loss products under different experimental conditions; Figure S-3, MS of Compound **3** with different ESI solvent compositions; Figures S-4 and S-5, EIMs of each isomer in several charge states; Figures S-6 and S-7, NETD fragmentation maps of each isomer ($[M - 3H]^{3-}$) following gated-TIMS separation; Figure S-8, zoomed-in regions of the NETD spectra of Compounds **3** and **4** ($[M - 3H]^{3-}$); Table S-1, typical instrument parameters used for gated-TIMS MS analysis; Tables S-2−S-6, lists of assigned peaks in the NETD spectra of each gated-TIMS-separated isomer; Table S-7, data used to generate the quantitative analysis plot shown in Figure 5 (PDF)

AUTHOR INFORMATION

Corresponding Author

*E-mail: chenglin@bu.edu.

DOI: 10.1021/acs.analchem.8b05283
Anal. Chem. 2019, 91, 2994−3001

ORCID

Catherine E. Costello: 0000-0003-1594-5122
Joseph Zaia: 0000-0001-9497-8701
Cheng Lin: 0000-0003-3653-9633

Author Contributions

C.L. defined the original concept. J. Wei and Y.T. performed the gated-TIMS MS/MS analysis. J. Wei and J. Wu performed spectral interpretation. M.E.R. and M.A.P. assisted with gated-TIMS implementation on FTICR MS. J. Wei and C.L. coordinated and wrote the manuscript with contributions from all authors. All authors have given approval to the final version of the manuscript.

Notes

The authors declare no competing financial interest.

■ ACKNOWLEDGMENTS

This research is supported by the NIH grants P41 GM104603, R21 GM122635, R21 CA199845, U01CA221234, and S10 RR025082 and National Natural Science Foundation of China (21728501). The authors thank Prof. Geert-Jan Boons for providing the synthetic GAG standards. The contents are solely the responsibility of the authors and do not represent the official views of the awarding offices.

■ REFERENCES

(1) Pomin, V. H. *Prog. Biophys. Mol. Biol.* **2014**, *114*, 61−68.
(2) Dam, G. B. t.; Kurup, S.; van de Westerlo, E. M. A.; Versteeg, E. M. M.; Lindahl, U.; Spillmann, D.; van Kuppevelt, T. H. *J. Biol. Chem.* **2006**, *281*, 4654−4662.
(3) Misek, D. E.; Patwa, T. H.; Lubman, D. M.; Simeone, D. M. *J. Natl. Compr. Cancer Network* **2007**, *5*, 1034−1041.
(4) Guerrini, M.; Beccati, D.; Shriver, Z.; Naggi, A. M.; Bisio, A.; Capila, I.; Lansing, J.; Guglieri, S.; Fraser, B.; Al-Hakim, A.; Gunay, S.; Viswanathan, K.; Zhang, Z.; Robinson, L.; Venkataraman, G.; Buhse, L.; Nasr, M.; Woodcock, J.; Langer, R.; Linhardt, R.; et al. *Nat. Biotechnol.* **2008**, *26*, 669−675.
(5) Wang, L.; Brown, J. R.; Varki, A.; Esko, J. D. *J. Clin. Invest.* **2002**, *110*, 127−136.
(6) Kelton, J. G.; Warkentin, T. E. *Blood* **2008**, *112*, 2607−2616.
(7) Yayon, A.; Klagsbrun, M.; Esko, J. D.; Leder, P.; Ornitz, D. M. *Cell* **1991**, *64*, 841−848.
(8) Turner, N.; Grose, R. *Nat. Rev. Cancer* **2010**, *10*, 116−129.
(9) Monneau, Y.; Arenzana-Seisdedos, F.; Lortat-Jacob, H. *J. Leukocyte Biol.* **2016**, *99*, 935−953.
(10) Mulloy, B.; Hogwood, J.; Gray, E.; Lever, R.; Page, C. P. *Pharmacol. Rev.* **2016**, *68*, 76−141.
(11) Weiss, R. J.; Esko, J. D.; Tor, Y. *Org. Biomol. Chem.* **2017**, *15*, 5656−5668.
(12) Bishop, J. R.; Schuksz, M.; Esko, J. D. *Nature* **2007**, *446*, 1030−1037.
(13) Petitou, M.; Casu, B.; Lindahl, U. *Biochimie* **2003**, *85*, 83−89.
(14) Jin, L.; Abrahams, J. P.; Skinner, R.; Petitou, M.; Pike, R. N.; Carrell, R. W. *Proc. Natl. Acad. Sci. U. S. A.* **1997**, *94*, 14683−14688.
(15) Pellegrini, L. *Curr. Opin. Struct. Biol.* **2001**, *11*, 629−634.
(16) Shriver, Z.; Capila, I.; Venkataraman, G.; Sasisekharan, R. *Handb. Exp. Pharmacol.* **2012**, *207*, 159−176.
(17) Zhao, Y.; Singh, A.; Xu, Y.; Zong, C.; Zhang, F.; Boons, G.-J.; Liu, J.; Linhardt, R. J.; Woods, R. J.; Amster, I. J. *J. Am. Soc. Mass Spectrom.* **2017**, *28*, 96−109.
(18) Kreuger, J.; Salmivirta, M.; Sturiale, L.; Giménez-Gallego, G.; Lindahl, U. *J. Biol. Chem.* **2001**, *276*, 30744−30752.
(19) Safaiyan, F.; Lindahl, U.; Salmivirta, M. *Biochemistry* **2000**, *39*, 10823−10830.
(20) Ruiz-Calero, V.; Moyano, E.; Puignou, L.; Galceran, M. T. *J. Chromatogr. A* **2001**, *914*, 277−291.
(21) Zamfir, A. D. *Electrophoresis* **2016**, *37*, 973−986.
(22) Sanderson, P.; Stickney, M.; Leach, F. E.; Xia, Q.; Yu, Y.; Zhang, F.; Linhardt, R. J.; Amster, I. J. *J. Chromatogr. A* **2018**, *1545*, 75−83.
(23) Melmer, M.; Stangler, T.; Premstaller, A.; Lindner, W. *J. Chromatogr. A* **2011**, *1218*, 118−123.
(24) Doneanu, C. E.; Chen, W.; Gebler, J. C. *Anal. Chem.* **2009**, *81*, 3485−3499.
(25) Gill, V. L.; Aich, U.; Rao, S.; Pohl, C.; Zaia, J. *Anal. Chem.* **2013**, *85*, 1138−1145.
(26) Miller, R. L.; Guimond, S. E.; Shivkumar, M.; Blocksidge, J.; Austin, J. A.; Leary, J. A.; Turnbull, J. E. *Anal. Chem.* **2016**, *88*, 11542−11550.
(27) Miller, R. L.; Guimond, S. E.; Prescott, M.; Turnbull, J. E.; Karlsson, N. *Anal. Chem.* **2017**, *89*, 8942−8950.
(28) Mosely, J. A.; Smith, M. J.; Prakash, A. S.; Sims, M.; Bristow, A. W. *Anal. Chem.* **2011**, *83*, 4068−4075.
(29) Lemmnitzer, K.; Riemer, T.; Groessl, M.; Sü*β*, R.; Knochenmuss, R.; Schiller, J. *Anal. Methods* **2016**, *8*, 8483−8491.
(30) Poyer, S.; Lopin-Bon, C.; Jacquinet, J. C.; Salpin, J. Y.; Daniel, R. *Rapid Commun. Mass Spectrom.* **2017**, *31*, 2003−2010.
(31) Schenauer, M. R.; Meissen, J. K.; Seo, Y.; Ames, J. B.; Leary, J. A. *Anal. Chem.* **2009**, *81*, 10179−10185.
(32) Kailemia, M. J.; Park, M.; Kaplan, D. A.; Venot, A.; Boons, G.-J.; Li, L.; Linhardt, R. J.; Amster, I. J. *J. Am. Soc. Mass Spectrom.* **2014**, *25*, 258−268.
(33) Seo, Y.; Andaya, A.; Leary, J. A. *Anal. Chem.* **2012**, *84*, 2416−2423.
(34) Seo, Y.; Schenauer, M. R.; Leary, J. A. *Int. J. Mass Spectrom.* **2011**, *303*, 191−198.
(35) Khanal, N.; Masellis, C.; Kamrath, M. Z.; Clemmer, D. E.; Rizzo, T. R. *Anal. Chem.* **2017**, *89*, 7601−7606.
(36) Agyekum, I.; Zong, C.; Boons, G.-J.; Amster, I. J. *J. Am. Soc. Mass Spectrom.* **2017**, *28*, 1741−1750.
(37) Wolff, J. J.; Amster, I. J.; Chi, L.; Linhardt, R. J. *J. Am. Soc. Mass Spectrom.* **2007**, *18*, 234−244.
(38) Wolff, J. J.; Chi, L.; Linhardt, R. J.; Amster, I. J. *Anal. Chem.* **2007**, *79*, 2015−2022.
(39) Huang, Y.; Yu, X.; Mao, Y.; Costello, C. E.; Zaia, J.; Lin, C. *Anal. Chem.* **2013**, *85*, 11979−11986.
(40) Leach, F. E.; Riley, N. M.; Westphall, M. S.; Coon, J. J.; Amster, I. J. *J. Am. Soc. Mass Spectrom.* **2017**, *28*, 1844−1854.
(41) Wolff, J. J.; Leach, F. E.; Laremore, T. N.; Kaplan, D. A.; Easterling, M. L.; Linhardt, R. J.; Amster, I. J. *Anal. Chem.* **2010**, *82*, 3460−3466.
(42) Wu, J.; Wei, J.; Hogan, J. D.; Chopra, P.; Joshi, A.; Lu, W.; Klein, J.; Boons, G.-J.; Lin, C.; Zaia, J. *J. Am. Soc. Mass Spectrom.* **2018**, *29*, 1262−1272.
(43) Oh, H. B.; Leach, F. E.; Arungundram, S.; Al-Mafraji, K.; Venot, A.; Boons, G.-J.; Amster, I. J. *J. Am. Soc. Mass Spectrom.* **2011**, *22*, 582−590.
(44) Shvartsburg, A. A.; Smith, R. D. *J. Am. Soc. Mass Spectrom.* **2007**, *18*, 1672−1681.
(45) Clowers, B. H.; Hill, H. H. *Anal. Chem.* **2005**, *77*, 5877−5885.
(46) Zucker, S. M.; Lee, S.; Webber, N.; Valentine, S. J.; Reilly, J. P.; Clemmer, D. E. *J. Am. Soc. Mass Spectrom.* **2011**, *22*, 1477.
(47) Hernandez, D. R.; DeBord, J. D.; Ridgeway, M. E.; Kaplan, D. A.; Park, M. A.; Fernandez-Lima, F. *Analyst* **2014**, *139*, 1913−1921.
(48) Michelmann, K.; Silveira, J. A.; Ridgeway, M. E.; Park, M. A. *J. Am. Soc. Mass Spectrom.* **2015**, *26*, 14−24.
(49) Adams, K. J.; Montero, D.; Aga, D.; Fernandez-Lima, F. *Int. J. Ion Mobility Spectrom.* **2016**, *19*, 69−76.
(50) Benigni, P.; Thompson, C. J.; Ridgeway, M. E.; Park, M. A.; Fernandez-Lima, F. *Anal. Chem.* **2015**, *87*, 4321−4325.
(51) Schenk, E. R.; Mendez, V.; Landrum, J. T.; Ridgeway, M. E.; Park, M. A.; Fernandez-Lima, F. *Anal. Chem.* **2014**, *86*, 2019−2024.
(52) Jeanne Dit Fouque, K.; Garabedian, A.; Porter, J.; Baird, M.; Pang, X.; Williams, T. D.; Li, L.; Shvartsburg, A.; Fernandez-Lima, F. *Anal. Chem.* **2017**, *89*, 11787−11794.

DOI: 10.1021/acs.analchem.8b05283
Anal. Chem. 2019, 91, 2994−3001

(53) Pu, Y.; Ridgeway, M. E.; Glaskin, R. S.; Park, M. A.; Costello, C. E.; Lin, C. *Anal. Chem.* **2016**, *88*, 3440−3443.
(54) Ridgeway, M. E.; Wolff, J. J.; Silveira, J. A.; Lin, C.; Costello, C. E.; Park, M. A. *Int. J. Ion Mobility Spectrom.* **2016**, *19*, 77−85.
(55) Benigni, P.; Porter, J.; Ridgeway, M. E.; Park, M. A.; Fernandez-Lima, F. *Anal. Chem.* **2018**, *90*, 2446−2450.
(56) Arungundram, S.; Al-Mafraji, K.; Asong, J.; Leach, F. E., III; Amster, I. J.; Venot, A.; Turnbull, J. E.; Boons, G.-J. *J. Am. Chem. Soc.* **2009**, *131*, 17394−17405.
(57) Ceroni, A.; Maass, K.; Geyer, H.; Geyer, R.; Dell, A.; Haslam, S. M. *GlycoWorkbench: A Tool for the Computer-Assisted Annotation of Mass Spectra of Glycans Journal of Proteome Research* **2008**, *7*, 1650−1659.
(58) Domon, B.; Costello, C. E. *Glycoconjugate J.* **1988**, *5*, 397−409.
(59) Håkansson, K.; Axelsson, J.; Palmblad, M.; Håkansson, P. *J. Am. Soc. Mass Spectrom.* **2000**, *11*, 210−217.
(60) Sannes-Lowery, K. A.; Hofstadler, S. A. *J. Am. Soc. Mass Spectrom.* **2000**, *11*, 1−9.
(61) Sannes-Lowery, K.; Griffey, R. H.; Kruppa, G. H.; Speir, J. P.; Hofstadler, S. A. *Rapid Commun. Mass Spectrom.* **1998**, *12*, 1957−1961.
(62) Liu, F. C.; Kirk, S. R.; Bleiholder, C. *Analyst* **2016**, *141*, 3722−3730.
(63) Zaia, J.; Li, X.-Q.; Chan, S.-Y.; Costello, C. E. *J. Am. Soc. Mass Spectrom.* **2003**, *14*, 1270−1281.
(64) Hitchcock, A. M.; Costello, C. E.; Zaia, J. *Biochemistry* **2006**, *45*, 2350−2361.
(65) Leach, F. E.; Arungundram, S.; Al-Mafraji, K.; Venot, A.; Boons, G.-J.; Amster, I. J. *Int. J. Mass Spectrom.* **2012**, *330*−*332*, 152−159.

DOI: 10.1021/acs.analchem.8b05283
Anal. Chem. 2019, 91, 2994−3001